A Cascaded Resonator Decoupling Network for Two Filtering Antennas

Jianfeng Qian, Benito Sanz Izquierdo, Steven Gao, *Fellow*, *IEEE*, Hanyang Wang, *Fellow*, *IEEE*, Hai Zhou, Huiliang Xu

***Abstract*—In this paper, a novel method for the decoupling between two filtering antennas is presented. The mutual coupling between two filtering antennas is investigated and a coupled-resonator decoupling network (DN) is developed. This coupled-resonator DN is co-designed with the coupled filtering antennas with little effect on the original filtering responses. By connecting this network to the coupled antennas in parallel, the mutual coupling between two 2nd order filtering antennas can be suppressed dramatically. A step-by-step realization of the DN is provided. To verify the concept, a prototype using the proposed DN was fabricated and measured. Full-wave simulations and measurements indicate that this coupled-resonator DN can enhance the isolation between two filtering antennas up to 30 dB without significantly affecting the filtering performance of each antenna, at a cost of 1.15 dB efficiency drop.**

***Index Terms*—Cascaded resonator, decoupling network, filtering antenna, in-band.**

I. Introduction

In recent years the integrated designs of different devices have drawn much attention among researchers and engineers. Through the co-design of filters and other RF devices, the system performance can be greatly improved [1-6]. Compared to a conventional scheme, a co-designed module usually shows more promising performance regarding cost, loss, and size.

Among these designs, one of the most interesting topics is filtering antenna. A filtering antenna/filtenna is an integrated module of filter and antenna, which is expected to be capable of filtering and radiating signals simultaneously. Many works in this field can be found in the literature [7-14]. Some of them have already found applications in the industry. Up to now, filtering antenna is not a fresh topic anymore. However, if a filtering antenna is used in a communication system, the mutual coupling problem must be considered. Thus, the study on the decoupling between two filtering antennas is necessary.

To suppress the mutual coupling (MC) between two identical antennas, many methods can be found in the literature, such as decoupling networks [16-21], physical placement [22], [23], multi-port feeding networks [24-26], and parasitic elements [27-31]. Most of these works are proposed for two identical antennas with limited decoupling bandwidths. Some of them also suffer from bulky structures, complicated physical implementation, or large element distances. Besides, according to the authors' knowledge, most of these methods have not been tested on the filtering antennas yet.

In this paper, a decoupling network for two filtering antennas is proposed. The network introduces an additional path between two antenna ports. To achieve stable decoupling throughout the band, the transmission coefficients of the coupling and decoupling paths should have the same magnitude but a 180° phase difference. The magnitude and phase behavior of the decoupling path is controlled by a coupled resonator network, which is more frequency-stable and compact than the conventional transmission line structure [18]. The DN can be synthesized according to the common filter theory, without affecting the impedance conditions of both antenna ports, thus maintaining the original filter function. This method offers many advantages such as flexible design, decoupling bandwidth, compact structure, and low cost. Most importantly, it enables the decoupling of two filtering antennas.

II. Physical Realization

A. Step 1: Unequal power dividing (PD) Network

Fig. 1 shows the structure of the filtering antenna for demonstration in this paper [11-13]. For the sake of generality and simplicity, a classical 2nd order resonator-fed aperture coupled filtering antenna is used as the test antenna. It consists of two substrates with a 2-mm air gap between them. The common ground plane is located on the upper surface of the bottom substrate. The feeding structures on the lower surface of the bottom substrate are then aperture coupled to the patch which is on the upper surface of the top substrate. The substrates used in this paper are all Rogers 4003 with a dielectric constant of 3.55 and a thickness of 0.813mm. The simulations are all carried out in the High Frequency Structure Simulator (HFSS) [32]. The response of this second-order filtering antenna is given in Fig. 1 (c). As can be seen, this antenna shows 2nd order filtering performance. The specifications for filtering antenna are given as follows: fractional bandwidth (FBW) = 6.1% (2.38 GHz – 2.53 GHz), centre frequency = 2.45 GHz, ripple level = 0.3 dB. This filtering antenna can be achieved by using a non-radiative resonator to feed a patch antenna. By adjusting the coupling strength between the resonator and patch, coupling of the port,

This work was supported by Huawei Technology Ltd.. (Corresponding author: Jianfeng Qian.)

J. F. Qian, and Benito Sanz Izquierdo are with the School of Engineering and Digital Arts, University of Kent, Canterbury CT2 7NT, U.K.

Steven Gao is with the Chinese University of Hong Kong, Hong Kong.

H. Zhou, H. Xu and H. Wang are with Huawei Technology Ltd..

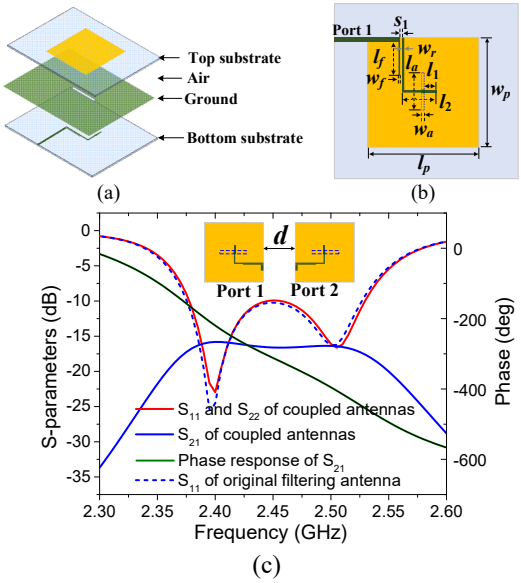

Fig. 1. Configurations of the filtering antenna. (a) Exploded view. (b) Top view. Dimensions in mm: l_1 = 5.04, l_2 = 12.75, l_a = 16.9, w_a = 1, l_f = 13.98, w_f = 0.4, S_1 = 0.35, l_p = 45.67, w_p = 45.5, w_r = 0.5. (c) Frequency responses for the filtering antenna under test and coupled antennas[1].

and patch dimensions, a 2nd order filter function can be obtained. The detailed design procedure of such a filtering antenna can be found in many works in the literature [11-13], so it is not given here for brevity.

Fig. 1 (c) provides the S-parameters when two identical filtering antennas are placed close to each other. The distance between the two patches is randomly set as 16.2 mm for generality, which is about 0.13 λ_0, where λ_0 is the free-space wavelength at the antenna's center frequency. It should be noted here that the proposed decoupling technique can also be used to decoupler antennas with smaller distances. For this case, the mutual coupling is about -16 dB in the operating band. It can be observed that the shape of the curve representing the mutual coupling (S_{21}) between these two antennas is very similar to the transmission coefficient of a lossy bandpass filter (BPF) [33].

To reduce the mutual coupling between two filtering antennas, the basic concept of our work is illustrated in Fig. 2 (a). As can be seen, a decoupling path is introduced parallelly with the coupling path between the antennas. To make sure the transmission from port1 to port 2 is perfectly suppressed, the transmission coefficients for both paths should have the same amplitude but 180-degree phase different, that is *Mag* (S_{MC})=*Mag* (S_{DN}) and $\angle(S_{MC}) = \angle(S_{DN}) + 180°$. Besides, to ensure a good decoupling performance in the whole operating band, the phase slopes of the transmission coefficients should be the same for both paths in the band of interest.

According to filter theory, the slope of the phase response for the coupling coefficient of a filtering circuit is related to its order and bandwidth [34]. Thus, the proposed decoupling network and coupled antennas should share the same bandwidth and filter order.

[1] Dashed line is simulated reflection coefficient of the original filtering antenna. Solid lines are the responses when two such antennas are coupled.

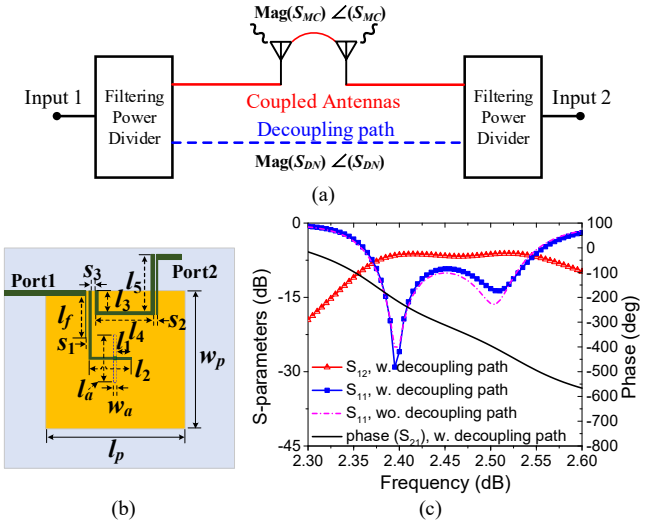

Fig. 2. (a) Conceptual framework of decoupled filtering antennas, (b) EM structure of the proposed filtering antenna with unequal PD and (c) S-parameters of the filtering antennas with/without decoupling path. Dimensions in mm: l_1 = 4.14, l_2 = 14.25, l_3 = 9.4, l_4 = 11.26, l_5 = 14.25,l_a = 17.09, w_a = 1, l_f = 13.98, w_f = 0.4, S_1 = 0.35, S_2 = 0.35, S_3 = 0.54, l_p = 45.62, w_p = 45.5.

To control the magnitude and phase of the decoupling path, the DN is separated into two identical blocks for ease of design. Fig. 2 (b) shows the basic block of the proposed decoupling structure. As can be observed, based on the structure shown in Fig. 1, another resonator is coupled to the first-stage resonator, dividing the energy into two parts. Fig. 2 (c) shows the frequency responses for the structure. This unequal power-dividing network shows almost the same S_{11} as the original filtering antenna. As the mutual coupling between original antennas is -16 dB, the insertion loss of the decoupling network (DN) should be 16 dB too. Thus, when the decoupling network is divided into two equal parts, the insertion loss from the driven port (port 1) to the decoupling port (port 2) in Fig. 2 (b) should be about 16/2=8dB. However, because of the inevitable loss of a coupled-resonator network, insertion loss of the decoupling path should be slightly lower than the mutual coupling level to compensate for the energy consumed in the decoupling network. As a result, the insertion loss for the decoupling path in Fig. 2 (b) is set as about 6.5 dB in our design.

B. Step 2: Construction of the Decoupling Path

In this step, two identical power-dividing (PD) networks obtained in *step 1* is combined to simulate the behavior of the coupled dual-antenna structure illustrated in Fig. 1 (c). To study the decoupling path solely, it is necessary to first eliminate the mutual coupling effect. This can be achieved by ensuring that the polarizations of the two antennas are orthogonal.

The dimensions of the DN can be decided through a curve-fitting procedure. The test structure for the establishment of DN is shown in Fig. 3. The proposed structure consists of two filtering antennas with the same filter function but orthogonal polarizations. This structure allows the study of the coupling dominated by the decoupling path. The coupling between the decoupling blocks is achieved by an aperture on the ground.

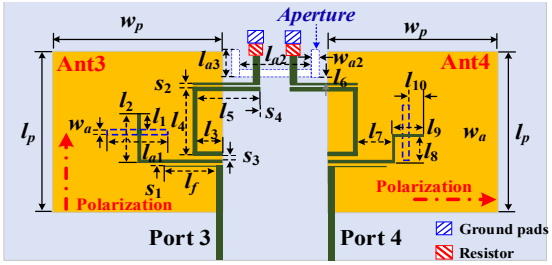

Fig. 3. Test structure used to find the decoupling path. Dimensions in mm: l_1 = 4.14, l_2 = 14.25, l_3 = 9.4, l_4 = 11.26, l_5 = 14.25, l_6 = 2.35, l_7 = 11.39, l_8 = 6.35, l_9 = 7.55, l_{a1} = 16.9, l_{a2} = 11.8, l_{a3} = 4, w_a = 1, l_f = 13.98, w_a = 1, w_{a2} = 0.8, l_f = 13.98, w_f = 0.4, S_1 = 0.35, S_2 = 0.35, S_3 = 0.54, S_4 = 0.72, l_p = 45.62, w_p = 45.5.

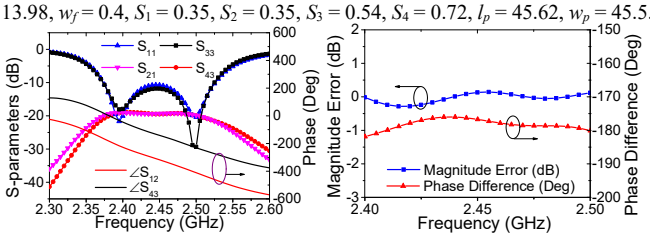

(a) (b)

Fig. 4. Simulated results of test structure and coupled antennas. (a) S-parameters. (b) Magnitude error and phase difference[2].

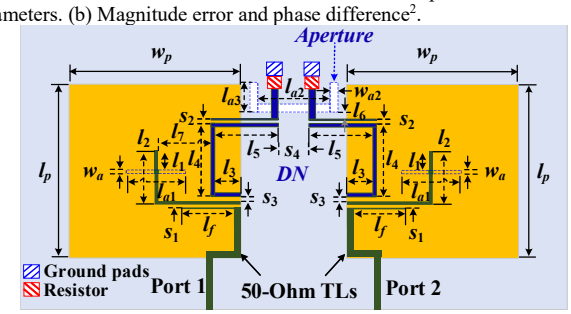

Fig. 5. Decoupled dual-filtenna structure for in-band application. Dimensions in mm: l_1 = 3.94, l_2 = 14.35, l_3 = 9.4, l_4 = 11.49, l_5 = 17.09, l_6 = 2.07, l_7 = 11.39, l_{a1} = 16.9, l_{a2} = 11.8, l_{a3} = 4, w_a = 1, w_{a2} = 0.8, l_f = 13.98, S_1 = 0.35, S_2 = 0.44, S_3 = 0.51, S_4 = 0.72, l_p = 45.67, w_p = 45.5.

Notably, the decoupling path is composed of four resonators, which is the same as the mutual coupling counterparts of the antennas, allowing for the matching of the slopes of the phase response of the two paths.

During the tuning process, the aperture's dimensions can be adjusted to control the magnitude of the transmission coefficient of the decoupling path, while the phase response should be carefully controlled to ensure that the decoupling path is out-of-phase with the coupled path between the original coupled antennas in the whole operating band. As the decoupling path shares the same filter function as the filtering antennas, the phase responses of the transmission coefficients for the original coupled antennas and the decoupling path are parallel to each other. In Fig. 4 (a), the magnitude and phase responses for both the test structure (S_{33}, S_{34}, $\angle(S_{34})$) and the original coupled antennas (S_{11}, S_{21}, $\angle(S_{12})$) are plotted and compared. As can be observed, despite some minor discrepancies, the magnitudes of the transmission coefficients for both structures agree well. The phase curves show similar trends too. Besides, a 180-degree phase difference can be

[2] S_{21} denotes the mutual coupling whereas S_{34} represents the decoupling path transmission coefficient. Magnitude error = $S_{21} - S_{43}$; Phase difference = $\angle S_{21} - \angle S_{43}$.

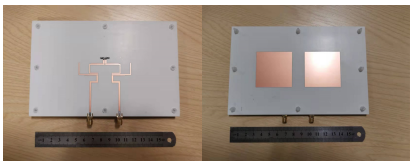

Fig. 6. Fabricated dual-antenna prototype for in-band operation.

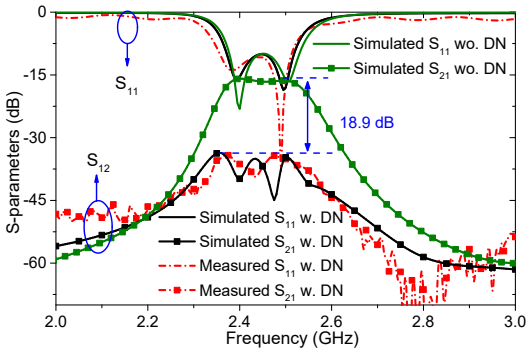

Fig. 7. Decoupling performance of the antennas.

observed. This phase shift is contributed to the external coupling structure which is realized by two coupled-transmission-line (CTL) sections [35]. Such a well-designed CTL structure can perform as an impedance inverter in the vicinity of the band of interest. Two additional inverters introduce the 180-degree phase difference we need.

Fig. 4 (b) illustrates the magnitude error and phase difference between the two paths. It is observed that the magnitude error can be tightly controlled within a narrow range of less than 0.27 dB in the band of interest. Additionally, the phase difference between the two paths falls within the range of 176-180 degrees. Using this method, the initial dimensions of the DN can be determined.

III. Experimental Demonstration and Discussion

In the last step, the realized decoupling network is connected with the dual-antenna module in parallel. After some finetuning, the final dimensions of the decoupled dual-antenna system can be determined as shown in Fig. 5.

A prototype was fabricated and measured for demonstration. Fig. 6 shows the photograph of the fabricated decoupled antennas. Fig. 7 presents the simulated and measured S-parameters. Despite some slight frequency shift, the antennas cover the 2.4 GHz WiFi band with a measured bandwidth of 2.36 GHz – 2.515 GHz. The decoupling network can improve the decoupling level up to 33.6 dB in simulation, which is about 34 dB in the measurement. Compared with the result given in Fig.1 (c), an improvement of 18.9 dB is achieved. In addition to achieving highly suppressed mutual coupling, this DN offers another significant advantage: it has minimal impact on the original S-parameters of the filtering antennas, as illustrated in Fig. 7. This feature is crucial for filtering antennas.

Fig. 8 plots the measured and simulated total radiation efficiencies of the decoupled filtering antenna [16]. Good filtering performance can be observed with respect to the out-of-band selectivity. A high roll-off rate on the skirt of the curve can be achieved by using a higher-order filter function.

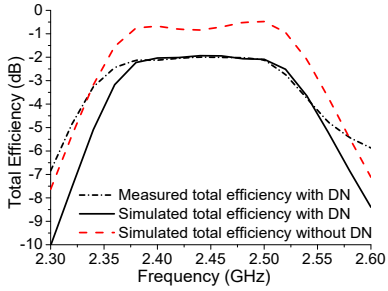

Fig. 8. The simulated and measured total efficiency of the dual-antenna system for in-band operation.

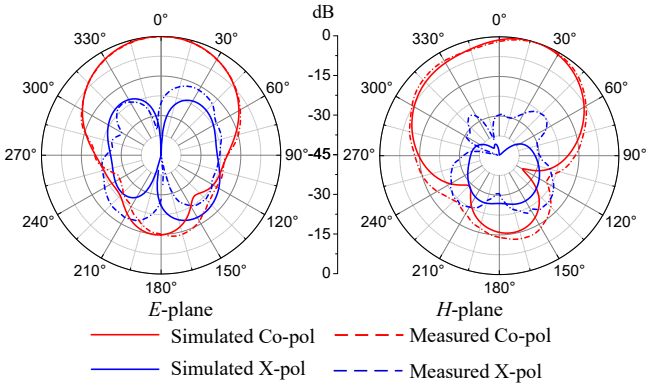

Fig. 9. Simulated and measured radiation patterns of the dual-antenna system for in-band operation.

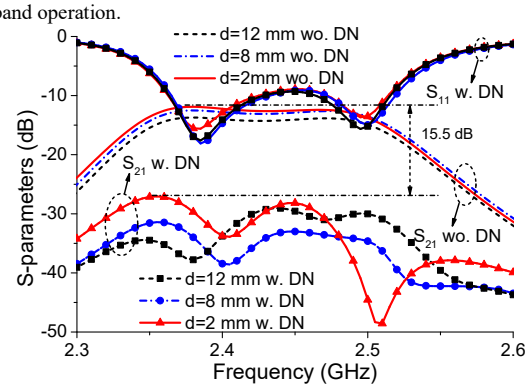

Fig. 10. Simulated decoupling performance with different antenna separations.

Also, as can be observed the measured total efficiency is about -1.94 dB in the band of interest. Our investigation revealed that the deterioration of total efficiency is about 1.15 dB at the center frequency of the antenna, which is slightly higher at the edges of the operating band (1.53 dB). This deterioration is primarily attributed to the resistors used in the structure. Our future work will focus on eliminating the losses in such coupled-resonator DNs. A possible direction will be designing DN using *Y*-parameter instead of *S*-parameters [17].

Fig. 9 shows the simulated and measured radiation patterns of the antennas for in-band application. Because of the symmetry of the structure, only the radiation patterns for one antenna are provided here. During the measurement, one antenna is excited while the other one is 50-Ohm terminated. The simulated and measured results agree well. The radiation pattern in its H-plane is slightly tilted from the broadside direction. This can be attributed to the reactive loading effect between two patches [36].

TABLE I. COMPARISON WITH PREVIOUS WORKS

Ref.	Edge-to-edge Spacing (λ_0)	Decoupling method	Iso. (dB)	Isolation improvement	TE (dB)	Filtering Response
[18]	N.G.	Network	29.1	>12.6dB	-4.7	No
[19]	0.12	Network	25.1	N.G.	-1.53	Yes
[20]	0.2	Network	32	14dB	-0.8	No
[30]	0.2	Decoupling surface	25	>15dB	N.G.	No
[31]	0.016	Near-field resonators	20	10dB	-0.9	No
This work	0.13	Filtering network	>30	18.9dB	-1.74	Yes

N.G.: Not given. λ_0: Free-space wavelength at the center frequency of the antenna; Iso.: Isolation; TE: total efficiency.

Table I shows the comparison of the performance between other presented works and this work. As can be observed, considering the edge-to-edge spacing, this work achieves a very competitive decoupling performance. Also, this work presents a possible solution for the decoupling between two filtering antennas. Although the decoupled antenna presented in [19] also has filtering ability, it suffers from limited application scenarios. Using the general method introduced in this work, many other decoupling problems between two resonating filtering antennas can be solved, but not limited to some specific antenna forms only. Besides, compared with another decoupling network presented in [18], the proposed method can achieve a more compact design. In this work, the phase behaviour is controlled by the coupled resonator, while in [18] a long transmission line and a phase shifter are needed for the adjustment of the phase response. Besides, two directional couplers are used in [18] for the power arrangement of the decoupling path which will also increase the cost and time of the design. However, by using coupled resonator decoupling network, our design provides a more general, cost-effective, and simpler solution for the decoupling between two filtering antennas. In this work, the distance between the two patches is about 0.13 λ_0. However, this distance could further be reduced to 0.02 λ_0 (2 mm) and still produce an improvement in isolation level of about 15.5 dB as shown in Fig. 10, which shows the decoupling performance with different antenna separations.

IV. CONCLUSION

This paper introduces a novel coupled resonator decoupling network for two filtering antennas. This network is developed based on the coupled-resonator filter theory. Step-by-step design procedures are provided in detail in this paper. For demonstration, a patch antenna prototype is fabricated and measured. The experimental and simulated results agree well. Compared with other presented works, this method shows a more flexible design, higher adaptability, and high decoupling performance. It should also be noted that theoretically this DN is not limited to the decoupling problem between patch antennas but can also serve for any other resonant antennas. These characteristics make it a good candidate for the decoupling between two filtering antennas.

REFERENCES

[1] X. Fang, Y. C. Li, Q. Xue *et al.*, "Dual-mode filtering baluns based on hybrid cavity-microstrip structures," *IEEE Transactions on Microwave Theory and Techniques,* vol. 68, no. 5, pp. 1637-1645, May 2020.

[2] J. Xu, H. Li, X. Y. Zhang *et al.*, "Compact dual-channel balanced filter and balun filter based on quad-mode dielectric resonator," *IEEE Transactions on Microwave Theory and Techniques,* vol. 67, no. 2, pp. 494-504, 2019.

[3] G. Shen, W. Che, W. Feng *et al.*, "High-isolation topology for filtering power dividers based on complex isolation impedance and surface wave suppression," *IEEE Transactions on Microwave Theory and Techniques,* vol. 69, no. 1, pp. 43-53, 2021.

[4] C.-F. Chen, J.-J. Li, G.-Y. Wang *et al.*, "Design of compact filtering 180-degree hybrids with arbitrary power division and filtering response," *IEEE Access,* vol. 7, pp. 18521-18530, 2019.

[5] J.-Y. Lin, Y. Yang, S.-W. Wong *et al.*, "Cavity filtering magic-t and its integrations into balanced-to-unbalanced power divider and duplexing power divider," *IEEE Transactions on Microwave Theory and Techniques,* vol. 67, no. 12, pp. 4995-5004, 2019.

[6] M. Akbarpour, M. Helaoui, and F. M. Ghannouchi, "Analytical design methodology for generic doherty amplifier architectures using three-port input/output networks," *IEEE Transactions on Microwave Theory and Techniques,* vol. 63, no. 10, pp. 3242-3253, 2015.

[7] Y.-M. Zhang, S. Zhang, G. Yang *et al.*, "A wideband filtering antenna array with harmonic suppression," *IEEE Transactions on Microwave Theory and Techniques,* vol. 68, no. 10, pp. 4327-4339, 2020.

[8] W. Duan, X. Y. Zhang, Y.-M. Pan *et al.*, "Dual-polarized filtering antenna with high selectivity and low cross polarization," *IEEE Transactions on Antennas and Propagation,* vol. 64, no. 10, pp. 4188-4196, 2016.

[9] K.-Z. Hu, M.-C. Tang, Y. Wang *et al.*, "Compact, vertically integrated duplex filtenna with common feeding and radiating siw cavities," *IEEE Transactions on Antennas and Propagation,* vol. 69, no. 1, pp. 502-507, 2021.

[10] Y. Li, Z. Zhao, Z. Tang *et al.*, "Differentially fed, dual-band dual-polarized filtering antenna with high selectivity for 5g sub-6 ghz base station applications," *IEEE Transactions on Antennas and Propagation,* vol. 68, no. 4, pp. 3231-3236, 2020.

[11] J. Qian, F. Chen, Y. Ding, H. Hu and Q. Chu, "A wide stopband filtering patch antenna and its application in MIMO system," *IEEE Transactions on Antennas and Propagation*, vol. 67, no. 1, pp. 654-658, Jan. 2019.

[12] C.-T. Chuang, and S.-J. Chung, "Synthesis and design of a new printed filtering antenna," *IEEE Transactions on Antennas and Propagation,* vol. 59, no. 3, pp. 1036-1042, 2011.

[13] C.-K. Lin, and S.-J. Chung, "A filtering microstrip antenna array," *IEEE Transactions on Microwave Theory and Techniques,* vol. 59, no. 11, pp. 2856-2863, 2011.

[14] R. H. Mahmud, M. J. Lancaster, "High-gain and wide-bandwidth filtering planar antenna array-based solely on resonators," *IEEE Trans. Antennas Propag.,* vol. 65, no. 5, pp. 2367-2375, May 2017.

[15] K. Iwamoto, M. Heino, K. Haneda *et al.*, "Design of an antenna decoupling structure for an inband full-duplex collinear dipole array," *IEEE Transactions on Antennas and Propagation,* vol. 66, no. 7, pp. 3763-3768, 2018.

[16] S. N. Venkatasubramanian, L. Li, A. Lehtovuori *et al.*, "Impact of using resistive elements for wideband isolation improvement," *IEEE Transactions on Antennas and Propagation,* vol. 65, no. 1, pp. 52-62, 2017.

[17] S.-C. Chen, Y.-S. Wang, and S.-J. Chung, "A decoupling technique for increasing the port isolation between two strongly coupled antennas," *IEEE Transactions on Antennas and Propagation,* vol. 56, no. 12, pp. 3650-3658, 2008.

[18] H. Makimura, K. Nishimoto, T. Yanagi *et al.*, "Novel decoupling concept for strongly coupled frequency-dependent antenna arrays," *IEEE Transactions on Antennas and Propagation,* vol. 65, no. 10, pp. 5147-5154, 2017.

[19] Y.-M. Zhang, Q.-C. Ye, G. F. Pedersen *et al.*, "A simple decoupling network with filtering response for patch antenna arrays," *IEEE Transactions on Antennas and Propagation,* vol. 69, no. 11, pp. 7427-7439, 2021.

[20] Y. Zhang, S. Zhang, J. Li *et al.*, "A transmission-line-based decoupling method for mimo antenna arrays," *IEEE Transactions on Antennas and Propagation,* vol. 67, no. 5, pp. 3117-3131, May 2019.

[21] L. Zhao, K. W. Qian, and K. L. Wu, "A cascaded coupled resonator decoupling network for mitigating interference between two radios in adjacent frequency bands," *IEEE Transactions on Microwave Theory and Techniques,* vol. 62, no. 11, pp. 2680-2688, Nov. 2014.

[22] H. Hu, F. Chen, and Q. Chu, "A compact directional slot antenna and its application in mimo array," *IEEE Transactions on Antennas and Propagation,* vol. 64, no. 12, pp. 5513-5517, 2016.

[23] Y. Luo, Q. Chu, J. Li *et al.*, "A planar h-shaped directive antenna and its application in compact mimo antenna," *IEEE Transactions on Antennas and Propagation,* vol. 61, no. 9, pp. 4810-4814, 2013.

[24] G. Makar, N. Tran, and T. Karacolak, "A high-isolation monopole array with ring hybrid feeding structure for in-band full-duplex systems," *IEEE Antennas and Wireless Propagation Letters,* vol. 16, pp. 356-359, 2017.

[25] E. A. Etellisi, M. A. Elmansouri, and D. Filipovic, "Broadband full-duplex monostatic circular-antenna arrays: Circular arrays reaching simultaneous transmit and receive operation," *IEEE Antennas and Propagation Magazine,* vol. 60, no. 5, pp. 62-77, 2018.

[26] Q. Xu, M. Biedka, and Y. E. Wang, "Indented antenna arrays for high isolation: The growing interest in simultaneous-transmit-and-receive-based full-duplex communication systems," *IEEE Antennas and Propagation Magazine,* vol. 60, no. 1, pp. 72-80, 2018.

[27] C.-Y. Chiu, C.-H. Cheng, R. D. Murch *et al.*, "Reduction of mutual coupling between closely-packed antenna elements," *IEEE Transactions on Antennas and Propagation,* vol. 55, no. 6, pp. 1732-1738, 2007.

[28] K. S. Vishvaksenan, K. Mithra, R. Kalaiarasan *et al.*, "Mutual coupling reduction in microstrip patch antenna arrays using parallel coupled-line resonators," *IEEE Antennas and Wireless Propagation Letters,* vol. 16, pp. 2146-2149, 2017.

[29] S. Hwangbo, H. Y. Yang, and Y. Yoon, "Mutual coupling reduction using micromachined complementary meander-line slots for a patch array antenna," *IEEE Antennas and Wireless Propagation Letters,* vol. 16, pp. 1667-1670, 2017.

[30] K.-L. Wu, C. Wei, X. Mei *et al.*, "Array-antenna decoupling surface," *IEEE Transactions on Antennas and Propagation,* vol. 65, no. 12, pp. 6728-6738, 2017.

[31] M. Li, B. G. Zhong, and S. W. Cheung, "Isolation enhancement for mimo patch antennas using near-field resonators as coupling-mode transducers," *IEEE Transactions on Antennas and Propagation,* vol. 67, no. 2, pp. 755-764, 2019.

[32] ANSYS HFSS, ANSYS Inc. [Online]. Available: http://www.ansys.com/Products/Electronics/ANSYS-HFSS

[33] V. Miraftab, and Y. Ming, "Advanced coupling matrix and admittance function synthesis techniques for dissipative microwave filters," *IEEE Transactions on Microwave Theory and Techniques,* vol. 57, no. 10, pp. 2429-2438, 2009.

[34] X. Guo, L. Zhu, and W. Wu, "Design of complex weighted feeding network based on generalized coupled-resonator filter theory," *IEEE Transactions on Microwave Theory and Techniques,* vol. 67, no. 11, pp. 4376-4385, 2019.

[35] E. M. T. Jones, "Coupled-strip-transmission-line filters and directional couplers," *IEEE Transactions on Microwave Theory and Techniques,* vol. 4, no. 2, pp. 6, April 1956.

[36] Y. Yusuf, and G. Xun, "A low-cost patch antenna phased array with analog beam steering using mutual coupling and reactive loading," *IEEE Antennas and Wireless Propagation Letters,* vol. 7, pp. 81-84, 2008.